

Frascati, March 29, 2010

Note: **IR-14****THE DAΦNE INTERACTION REGION FOR THE KLOE-2 RUN***C. Milardi, M. Preger, P. Raimondi***Introduction**

Recently a new collision scheme based on large Piwinski angle and Crab-Waist compensation of the beam-beam interaction [1] has been proposed and implemented [2] on DAΦNE [3]. The new configuration has been used to provide beam-beam events to the SIDDHARTA [4] experiment, a compact device without solenoidal field, heir of DEAR, providing a simple environment for the *Crab-Waist* test. The luminosity has been increased by a factor 3 with a peak value of  $4.53 \times 10^{32} \text{ cm}^{-2} \text{ s}^{-1}$  letting in collision currents slightly lower than those corresponding to the old records. The highest daily integrated luminosity measured in a moderate injection regime, suitable for SIDDHARTA operation, has been  $L_{\text{fday}} \sim 15 \text{ pb}^{-1}$ . An almost continuous injection regime provided  $L_{\text{f1 hour}} \sim 1.0 \text{ pb}^{-1}$  hourly integrated luminosity which opened significant perspectives for the KLOE-2 experiment. Scaling this best integrated luminosity measured over two hours, it is reasonable to expect more than  $20 \text{ pb}^{-1}$  per day, and assuming 80% collider uptime as during the past runs,  $\sim 0.5 \text{ fb}^{-1}$  per month [5].

The results of the high luminosity test have renovated the interest about the experimental activity on the DAΦNE collider, paving the way for a new run with an upgraded KLOE detector, KLOE-2.

**1 KLOE and KLOE-2**

KLOE [6] is a multipurpose experiment devoted, mainly, to the study of K meson decays, as well as to several hadronic physics and low energy quantum chromodynamics studies. The detector consists of a large cylindrical drift chamber,  $\sim 3.5 \text{ m}$  long and  $2 \text{ m}$  radius, surrounded by an electromagnetic calorimeter of lead and scintillating fibers. A superconducting coil around the detector provides a magnetic field of  $0.52 \text{ T}$ .

With respect to the original design, KLOE-2 [7] introduces few well defined modifications: additional detector layers, including both tracking and calorimeter devices, have been inserted in the inner part of the apparatus, close to the interaction region. A very light tracker, consisting of a cylindrical GEM detector, has been installed in the space between the drift chamber and the spherical beam pipe. Crystal calorimeters, in front the collider low- $\beta$  quadrupoles, will increase the acceptance for photons emitted under a very low angle, a key issue for some rare decay studies. KLOE-2 will also extend its investigation capabilities to the study of  $\gamma\text{-}\gamma$  reactions, by means of dedicated detectors tagging the scattered electron and positron, typical of those events.

**2 The DAΦNE Interaction Region for the KLOE-2 run**

Integrating the high luminosity collision scheme with the KLOE-2 detector introduces new challenges in terms of IR layout and optics, beam acceptance and coupling correction.

## 2.1 IR Layout

The low- $\beta$  section is based, as for the SIDDHARTA configuration, on permanent magnet quadrupole doublets. The quadrupoles are made of SmCo alloy and provide gradients of 29.2 T/m for the first one from the IP and 12.6 T/m for the second one. The first (PMQD) is horizontally defocusing and is shared by the two beams; its central azimuthal position has been set at 0.415 m from the IP (0.415) m, as a compromise between the conflicting requirements of tight focusing and large solid angle aperture coming from the collider and the experiment respectively. The second quadrupole (PMQF), horizontally focusing, is installed just after the point where the beam pipes of the two rings are separated and is therefore on axis. Being PMQD much stronger than in the old KLOE low- $\beta$  setup and having doubled the horizontal half crossing angle, now  $\sim 25$  mrad, a very efficient beam separation is achieved in the  $\sim 1.6$  m long section of the IR common to the two rings, making the impact of a single parasitic crossing completely negligible. As a drawback the vertical displacement of the beam in the IR, which is also affected by the detector solenoidal field, becomes an order of magnitude larger than in the past KLOE run. To keep the beam vertical trajectory within reasonable values a permanent magnet dipole, PMD, has been added just after PMQF, inside the detector magnetic field, in each one of the four IR branches. Each PMD is built by using a SmCo alloy, consists of two parts having 75.0 mm magnetic length each, and provides an integrated field strength  $BL = 0.0168$  Tm corresponding to a vertical deflection angle of  $\sim 10.0$  mrad. The PMDs are based on a modular design in view of a possible KLOE-2 run at a lower solenoidal field. They provide a horizontal magnetic field directed inward in the  $e^+$  ring and outward in the  $e^-$  one, as shown in Fig. 8.

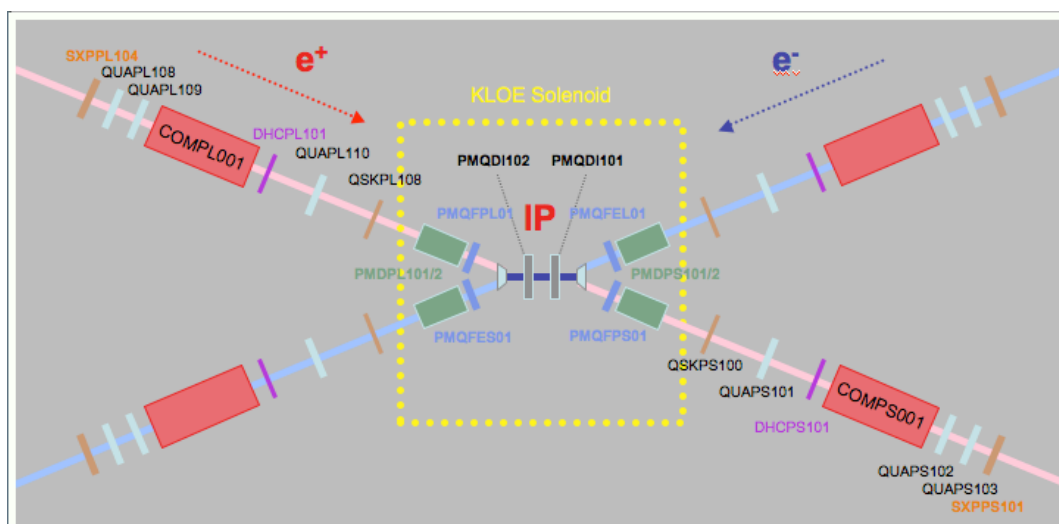


Figure 1: Schematic drawing of the DAΦNE Interaction Region for the KLOE-2 run.

The IR magnetic layout, sketched in Fig. 1, has been designed in order to maximize the beam stay clear letting the beam trajectory pass as much as possible through the center of the magnetic elements according to a self-consistent procedure which, for symmetry reasons, has been developed for one section of the IR only. The crossing angle has been tuned in order to have the same horizontal displacement as in the SIDDHARTA configuration at the corrector dipole,

DHCPS01, used to match the IR to the ring layout in the arcs, under the constraint of placing the PMDs as close as possible to the PFQMs; its value ( $\theta_c = 25.7$  mrad) has been computed switching off PMQFPS01 and the electromagnetic quadrupole QUAPS101 before DHCPS01. The  $x, x', y, y'$  coordinates of PMQFPS01 have been calculated, imposing that the  $x, y$  beam trajectory remains constant at DHCPS01 with or without PMQFPS01 itself. The QUAPS101 quadrupole is slightly displaced with respect to the beam in order to compensate the small steering due to the practical constraint of leaving it in the upright position for alignment reasons. Eventually the DHCPS101 dipole has been used to steer the beam trajectory through the center of the compensator solenoid COMPS001.

The beam trajectory and positions of the magnetic element center positions are shown in Fig. 2 and in Fig. 3 with reference to the IR branch of the positron ring pointing to the short arc, the corresponding branch for the electron ring being symmetric.

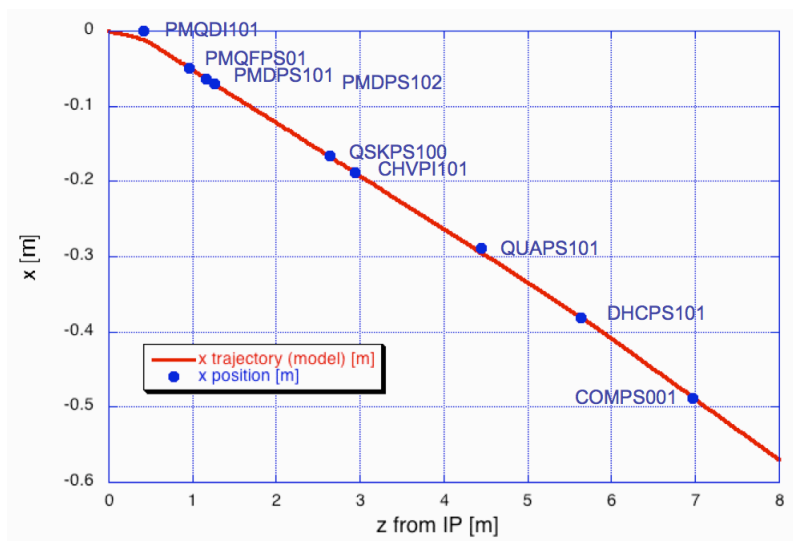


Figure 2: Horizontal trajectory in the IR (solid line) and position of the IR magnetic element centers (dots).

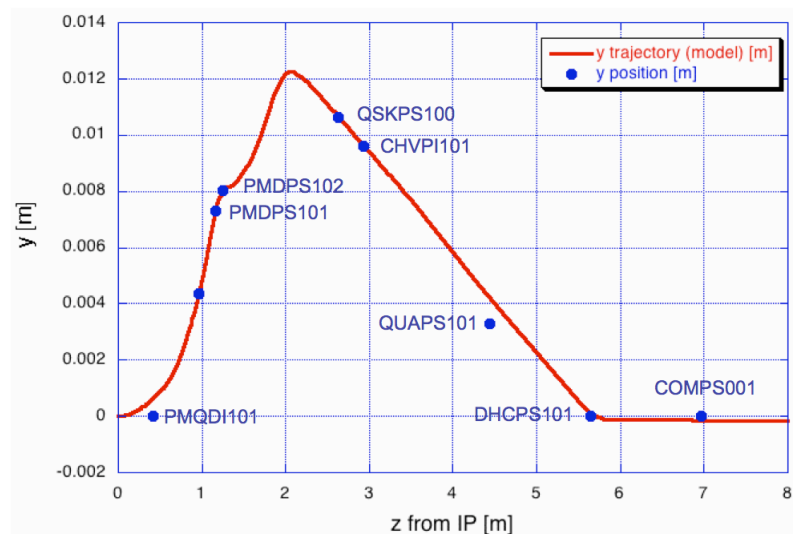


Figure 3: Vertical trajectory in the IR (solid line) and position of the IR magnetic element centers (dots).

The small contribution to the vertical beam deflection coming from the beam passing off-axes in the QUAPS101 is comparable with the alignment tolerance.

The evident advantage of this approach consists in keeping the maximum excursion of the vertical beam trajectory within  $\sim 12$  mm providing, at the same time, the maximum aperture for the beam.

The horizontal and vertical beam stay-clear requirements have been defined as:

$$X_{SC} = x_{trj} \pm 10\sigma_x$$

$$Y_{SC} = y_{trj} \pm 10\sigma_y$$

where  $\sigma_x$  and  $\sigma_y$  are the horizontal and vertical rms beam sizes respectively. Their values, computed with the collider emittance  $\varepsilon = 0.4 \cdot 10^{-6}$  m for the horizontal plane and full coupling for the vertical one, are presented in Fig. 4 and Fig. 5. Relying on this analysis the radius of the vacuum pipe, in the section between the IP and the DHC, has been reduced. It is now 2.75 cm, while it was 4.4 cm during the SIDDHARTA run. A narrower vacuum chamber contributes to lower the ring impedance budget, to minimize the strength of trapped High Order Modes and to shift their frequencies away from the beam spectral lines. The resulting vacuum pipe geometry is largely simplified; in fact it consists of three straight sections, with few junctions and bellows. The detector efficiency also profits from the larger free space around the IP where a precision vertex tracker can be placed.

The IR pipe is aluminum (AL6082) made with the exception of the sphere surrounding the IP, which is built in ALBEMET. Such a structure could trap HOMs and for this reason it is shielded from the beam by means of a Be cylinder. To minimise K meson regeneration the shield thickness has been almost halved ( $35 \mu$  instead of the  $65 \mu$  of the last KLOE run).

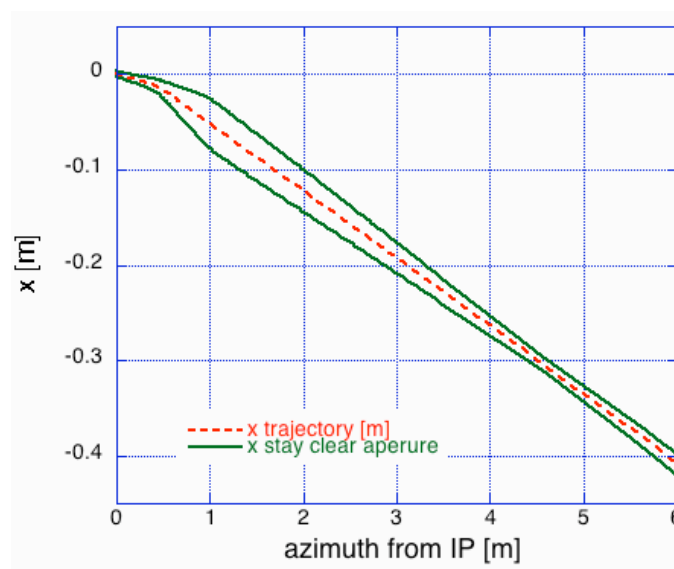


Figure 4: Horizontal beam stay-clear aperture in the KLOE-2 IR.

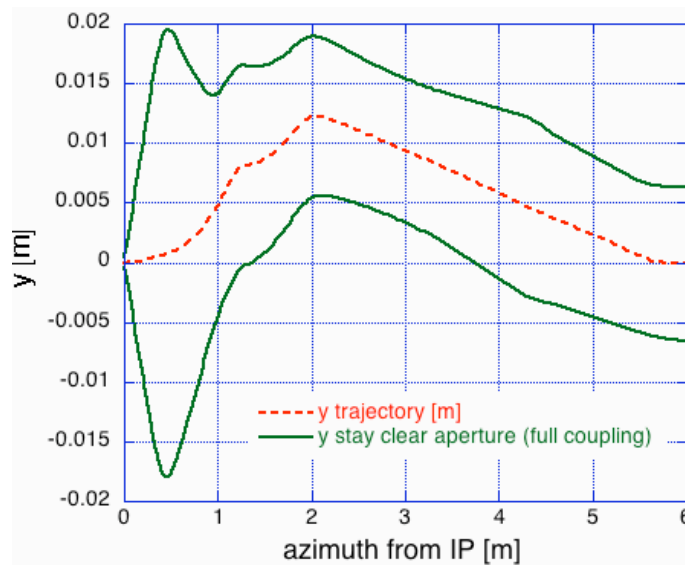


Figure 5: Vertical beam stay-clear aperture in the KLOE-2 IR.

## 2.2 IR Optics

The design of the IR optics is constrained by several criteria. It must provide the prescribed low- $\beta$  parameters at the IP (see Tab. 1), matching at the same time the ring original layout in the arcs. The phase advance between the Crab-Waist Sextupoles and the IP must be  $\pi$  for the horizontal-like mode and  $\pi/2$  for the vertical one. The value of the  $\beta$ -functions at the Crab-Waist Sextupoles must be tuned to the values that fully exploit the strength of the existing devices. The transverse coupling introduced by the detector solenoid must be carefully compensated by means of the compensator solenoids and rotation of the IR quadrupoles.

Table 1: Interaction region parameters

$\beta_x$ [m]	0.265
$\beta_y$ [m]	0.0085
$ \theta_c $ (half value) [rad]	0.0257
$\alpha_x$	0.0
$\alpha_y$	0.0
$\eta_x$ [m]	0.0
$\eta'_x$	0.0

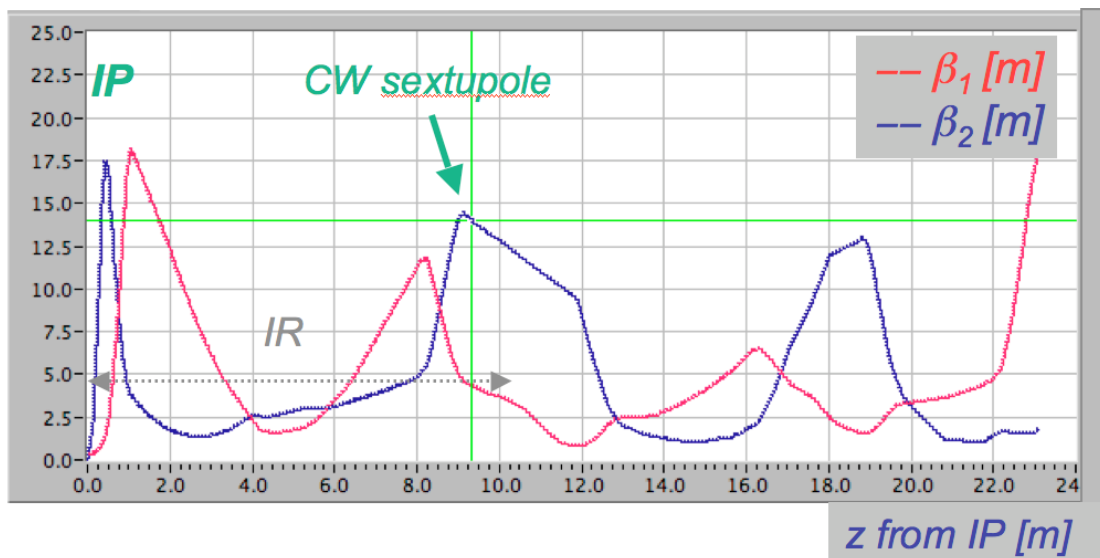


Figure 6: IR optical functions.

### 2.3 Coupling correction

The transverse betatron coupling has been corrected revising the Rotating Frame Method [8] originally used at DAΦNE. The field integral introduced by the solenoidal detector is almost cancelled by means of two anti-solenoids, installed symmetrically with respect to the IP in each ring, which provides compensation also for off-energy particles. The rotation of the beam transverse plane is compensated by coo-rotating the quadrupoles PMQFPS01, QUAPS101, QUAPS102, QUAPS103 around their longitudinal axis. The first low beta quadrupole has been kept in the upright position, achieving a reasonable compromise between the conflicting requirements of keeping the vertical trajectory within reasonable limit and coupling correction (see Fig. 7). The anti-solenoidal field has been set to a value slightly lower with respect to the optimal one in order to minimize the rotation angles and to make the tilts corresponding to the last two electromagnetic quadrupoles symmetric. It is worth remarking that the coupling is carefully compensated before the CW sextupoles making the terms of the coupling matrix vanish at QUAPS103.

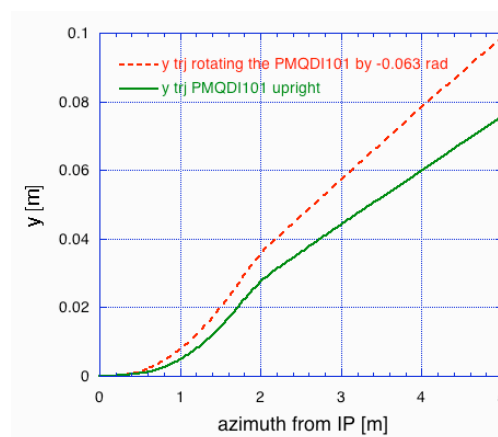


Figure 7: Dependence of the beam vertical trajectory on the nominal rotation of PMQD around its longitudinal axis.

Coupling correction fine-tuning, for each beam, is assured by a skew quadrupole added in each branch of the IR and by the two anti-solenoids independently powered.

The present coupling correction method introduces several advantages with respect to the one adopted for the past KLOE run. The rotation of the permanent magnet quadrupoles installed inside the detector is drastically reduced; in fact it was 8.3 deg and 12.9 deg for PMQD and PMQF respectively. Moreover it becomes possible to get rid of the remotely controlled actuators [9] used in the past to finely adjust the low- $\beta$  quadrupole tilts, thus further increasing the solid angle available for the detection of decaying particles. Quadrupole rotations in the four sections of the IR are summarized in Fig. 8. They are defined so that a positive tilt gives a clockwise rotation in the reference system moving with the positron beam.

A residual coupling in the range  $\kappa = 0.2\% \div 0.3\%$ , as in the past KLOE run is expected to be reached by this approach. The IR parameters are summarized in Tab. 2.

Table 2.

	Z from the IP [m]	Quadrupole rotation angles [deg] <i>Anti-solenoid current [A]</i>
PMQDI101	0.415	0.0
PMQFPS01	0.963	-4.48
QSKPS100	2.634	used for fine tuning
QUAPS101	4.438	-13.73
QUAPS102	8.219	0.906
QUAPS103	8.981	-0.906
COMPS001	6.963	72.48 ( <i>optimal value 86.7</i> )

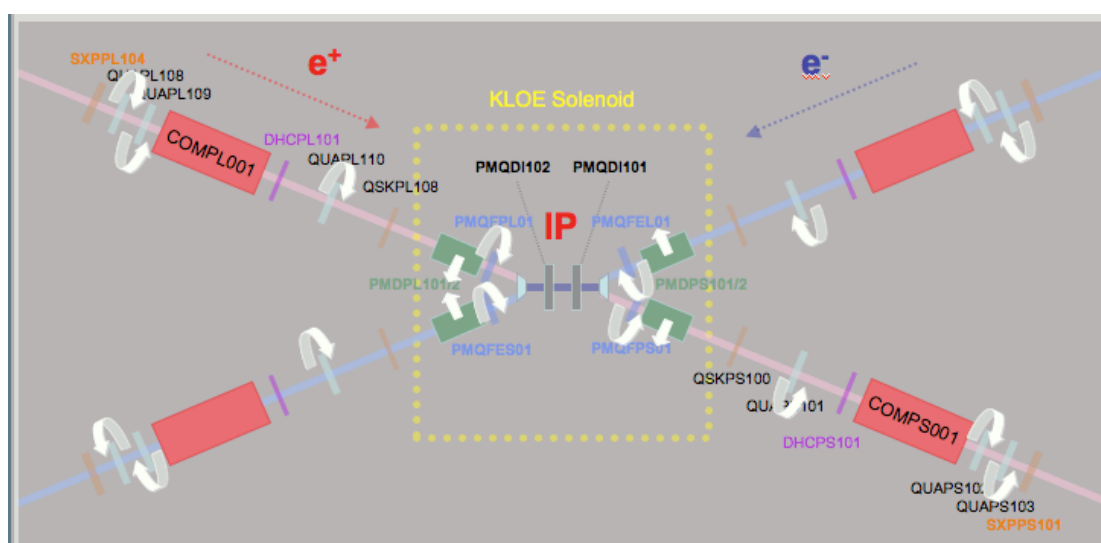


Figure 8: Quadrupole tilts for transverse coupling correction and direction of the horizontal magnetic field generated by the system of permanent dipole magnets.

## Conclusions

The eight permanent magnet dipoles have been designed and built; they are presently in the Frascati LNF laboratory ready to be installed.

Transverse coupling correction has been fully calculated.

The IR optics has been designed in order to fulfill all the requirements in terms of low beta functions at the IP, coupling correction and inclusion of the crab sextupoles. Tracking studies have been performed to ensure compatibility of the IR new structure with the mechanical layout of the ring arcs.

The IR vacuum chamber mechanical design has been completed and all the parts are under delivery.

In the next months the efforts will be addressed to define and optimize the DAΦNE main rings optics including the new IR, as well as to perform simulation studies about beam dynamics, beam-beam and backgrounds hitting the experimental detector.

## Acknowledgements

Work funded by the EuCARD research programme, within the "Assessment of Novel Accelerator Concepts" work package (ANAC-WP11).

## References

- [1] P. Raimondi, D. Shatilov, M. Zobov, physics/0702033.
- [2] C. Milardi et al., arXiv:0803.1450v1 [physics.acc-ph].
- [3] G. Vignola et al., Frascati Phys. Ser. 4:19-30, 1996.
- [4] SIDDHARTA Collab., Eur. J. Phys. A 31 (2007) 537-539.
- [5] C. Milardi et al., Vancouver 2009, PAC09, MO4RAI01.
- [6] KLOE Collab., Nucl. Inst. Meth. A 482, 363-385 (2002).
- [7] F. Bossi, The KLOE-2 project, Journal of Physics: Conference Series 171 (2009) 012099.
- [8] M. Bassetti et al., Frascati Series Vol. X (1998), pg. 209, 14<sup>th</sup> Advanced ICFA BD Workshop, Frascati, 1997.
- [9] C. Milardi et al., EPAC04, 233-235.